TARGET SHAPE CLASSIFICATION USING ELECTROMAGNETIC INDUCTION SENSOR DATA

Nagi Khadr
Bruce J. Barrow
Thomas H. Bell
AETC, Inc.
1225 Jefferson Davis Highway, Suite 800
Arlington, VA 22202
(703) 413-0500 • fax (703) 413-0512
nagi@va.aetc.com • bjb@va.aetc.com • tbell@va.aetc.com

Herbert H. Nelson
Naval Research Laboratory
Chemistry Division, Code 6110
Washington, DC 20375-5342
(202) 767-3686 • fax (202) 404-8119
herb.nelson@nrl.navy.mil

ABSTRACT

Classification based on shape is central to the problem of discriminating between unexploded ordnance (UXO) and clutter. Most UXO fit a specific profile: they are long and slender with typical length-to-diameter aspect ratios of four or five. Most clutter items, on the other hand, do not fit this profile. Using electromagnetic induction (EMI) sensor data, we present a model-based estimation procedure to determine whether or not a target is likely to be a UXO item. The model relies on exploiting the dependence of the induced field on target size, shape and orientation. Carefully collected measurements using a modified EM61 from the Naval Research Laboratory (NRL) Multi-sensor Towed Array Detection System (*MTADS*) are used to establish this dependency.

INTRODUCTION

Often as many as 95% of suspected anomalies encountered in buried UXO remediation efforts are not UXO. The result is that about 70% of the remediation cost goes towards the excavation of objects which could have been left in the ground [1]. In this paper, we describe recent work undertaken to address the issue of discriminating between buried UXO and clutter using time domain EMI sensors. This represents a joint effort by AETC and NRL as part of an Environmental Security Technology Certification Program (ESTCP) demonstration project.

Most ordnance items are long and slender, with typical length-to-diameter aspect ratios of four or five. Many clutter items which are detected in UXO surveys have markedly different shapes than this. We have shown previously that the EMI response of an ordnance item is significantly different depending on whether the primary field is aligned with the long axis of the target or perpendicular to it. Furthermore, the strength and spatial pattern of the EMI signal is very well represented by a model based on the magnetostatic induced dipole moment for a permeable prolate spheroid [2].

By recognizing the significance of this result for target classification, we are currently developing a parametric model which relates the properties of an *effective* magnetic polarizability tensor to physical attributes of the target. This tensor essentially acts as the constant of proportionality between the sensor response and the peak primary field, and incorporates details of the EMI sensor (such as the transmitter pulse and receiver time gate characteristics) with the frequency dependent magnetic polarizability tensor. The advantage of using such a tact is that it provides simple analytical expressions where none existed by reducing the dimensionality of the problem, and in the process makes it more suitable for optimization purposes.

To assist in the model development, measurements have been taken with one of the *MTADS* modified EM61 sensors. We provide a description of the measurement process and show some of the data acquired. Finally, preliminary results on parameter estimations and their associated minimum χ^2 surfaces are discussed.

EM61 RESPONSE MODEL

The EM61 is a time domain instrument. It operates by transmitting a magnetic pulse which induces currents in any nearby conducting objects. These currents produce

secondary magnetic fields which are measured by the sensor after the transmitter pulse has ended. The sensor response is the voltage induced in the receiver coil by these secondary fields, and is proportional to the time rate of change of the magnetic flux through the coil. The sensor integrates this induced voltage over a fixed time gate and averages over a number of pulses.

Our model relies upon the fact that the EM61 signal is a linear function of the flux through the receiving coil. The flux is assumed to originate from an induced dipole moment at the target location given by

$$\mathbf{m} = UBU^T \cdot \mathbf{H_o} \qquad (1)$$

where $\mathbf{H_o}$ is the peak primary field at the target, U is the transformation matrix between the coordinate directions and the principal axes of the target, and B is the effective magnetic polarizability tensor. This tensor contains information about the target (i.e. size, shape and composition), as well as the details of the EM61 (i.e. transmitter pulse and receiver time gate characteristics).

For a prolate spheroid, B is a diagonal tensor with only two unique coefficients, corresponding to the longitudinal (β_l) and transverse (β_t) directions:

$$B = \begin{pmatrix} \beta_l & 0 & 0 \\ 0 & \beta_t & 0 \\ 0 & 0 & \beta_t \end{pmatrix} \qquad (2)$$

In the static limit, these coefficients reduce to the magnetostatic polarizabilities for a prolate spheroid [3].

INDUCED FIELD RATIOS

In order to obtain information on target shape, it is helpful to examine the ratio of the axially induced field (i.e. the field induced based on the component of the primary field along the longitudinal axis of the target, or equivalently β_l) to the transversely induced field (i.e. β_t). Analytic expressions for the magnetostatic polarizabilities for permeable prolate spheroids indicate a direct relationship between this ratio and the length-to-diameter aspect ratio of targets. The question is whether these relationships are still valid when the effects of the sensor, along with the frequency dependence of the polarizabilities, are included. The answer is suggested by the data gathered to date (see Figure 1).

Each symbol in Figure 1 represents a target. Ordnance items are designated by the square and diamond symbols; test objects by the triangle symbol; and clutter items by the cross symbol. The two clutter items that are out on their own are non-permeable (aluminum); all the other targets are permeable (iron or steel).

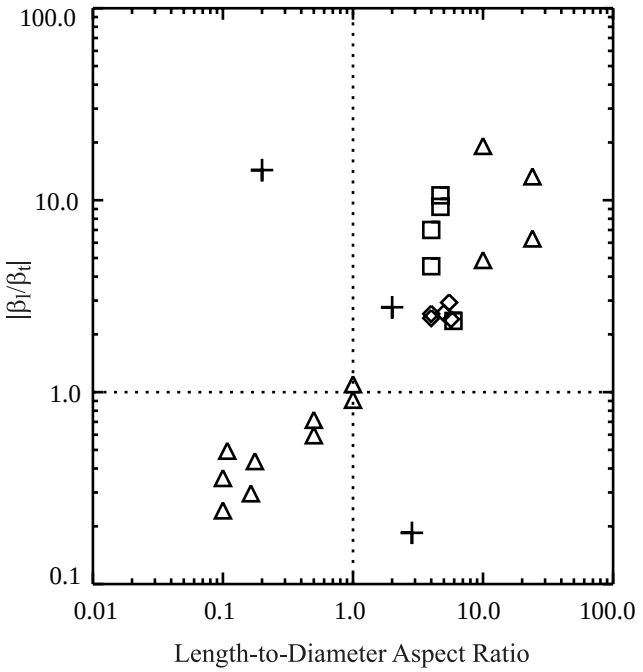

Figure 1. The induced field ratio for UXO (squares), clutter (crosses) and test objects (triangles) obtained via a modified EM61. The diamonds also represent UXO, but these were obtained via a standard EM61.

The results of Figure 1 are encouraging. They show that for permeable targets, if the target is long and slender about an axis of symmetry, the induced field ratio is greater than 1; if not, the ratio is 1 or less. For the only two non-permeable targets, the inverse seems to hold.

The scatter among the items is mainly due to the combined effects of differences in the size, shape and composition of the individual pieces. To assist in the development of a parametric model which relates these physical attributes of the target to the effective magnetic polarizability tensor coefficients, we turn to carefully collected EMI measurements.

EM61 MEASUREMENTS

A series of EMI measurements were obtained using one of the modified EM61 sensors from the NRL *MTADS* platform. These measurements were collected for UXO,

clutter, and a number of test objects. The objects are listed in Table 1.

By varying the location and orientation of the transmitter coil, it is possible to examine each object from different perspectives. In order to exhaust all perspectives, we have collected spatial measurements with three mutually orthogonal coil orientations.

In its intended mode of operation, the EM61 transmitter coil lays flat about 40cm above the ground. The lower receiver coil (R_2) is co-located with the transmitter coil (T), and the upper receiver coil (R_1) is about 40cm above this. In order to designate this particular configuration, we use the label Transmitter-Bottom (T-B). The remaining two mutually orthogonal coil orientations are then Transmitter-North (T-N) and Transmitter-West (T-W) depending on the direction of the transmitter coil relative to the offset receiver (refer to Figure 2).

Object Type	Description	D (m)	L (m)
UXO	2.75" Rocket	0.070	0.330
Clutter	Flattened Soda Can	~0.10	~0.02
	Shovel Blade	-	-
	Tail Fin Assembly	0.081	0.230
	Clump of Banding Material	~0.15	~0.30
Test Object	Sphere	0.124	0.124
	Cylinder	0.038	0.381
		0.019	0.190
		0.025	0.610
		0.013	0.305
	Disk	0.152	0.076
		0.076	0.038
		0.152	0.015
		0.076	0.008

Table 1. A list of objects, with relevant dimensions, for which careful spatial EM61 measurements were obtained. D and L represent the diameter and length, respectively.

The method by which spatial measurements were obtained was by placing an object directly below the center of the transmitter coil for each sensor configuration as shown in Figure 2, gathering data for about a 30s interval, and incrementally moving the object in a southward direction, each time stopping to gather data. This was repeated three times for each object, with the long axis (or more accurately, the axis of symmetry) of the object facing in a different mutually orthogonal direction each time: East (E),

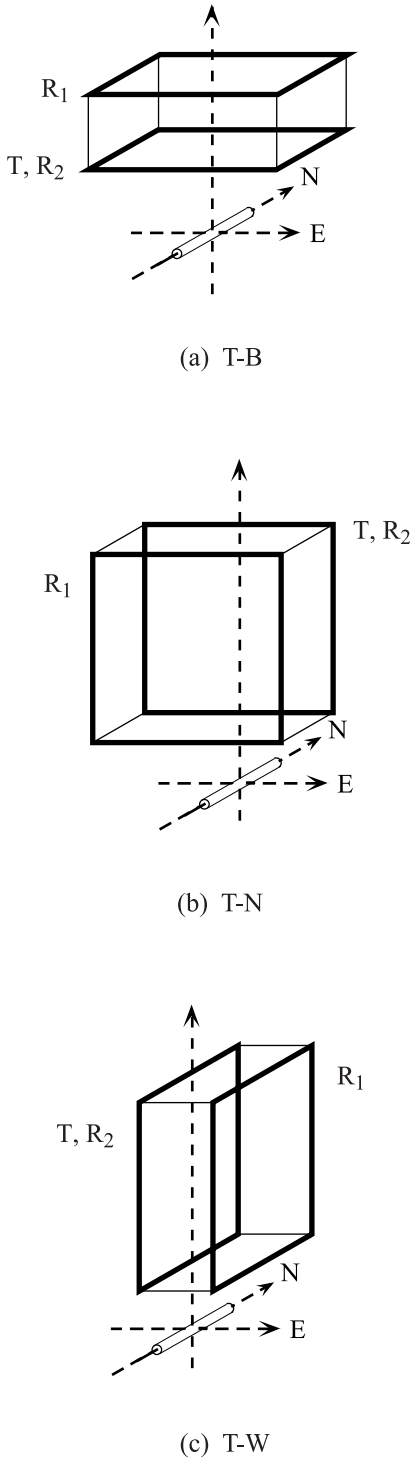

Figure 2. Configuration of three mutually orthogonal coil orientations and their chosen designators: (a) Transmitter-Bottom; (b) Transmitter-North; and (c) Transmitter-West.

North (N) and vertical. A photograph of the measurement apparatus is provided in Figure 3.

Figure 3. The measurement apparatus showing a modified *MTADS* EM61 sensor in the T-N configuration collecting spatial data for a small vertical cylinder.

RESULTS AND DISCUSSION

As an example, Figure 4 shows the spatial data collected for the 2.75" rocket (long axis facing northwards) with the three respective sensor configurations of Figure 2. The symbols represent the measured averaged values; the solid lines represent the best model fit using a χ^2 minimization procedure. The shaded regions show the consequence of varying the β_l and β_t parameters by as much as ±20%.

The χ^2 minimization procedure entails fitting the response model of (1) and (2) to all six data channels simultaneously. Here, χ^2 is proportional to the sum of the squared differences between model and measurement over all data points, a figure of merit commonly used to quantify how well a model fits the data. Thus, the lower the χ^2, the better the fit.

A glance at the relative signal levels of R_2 (i.e. the receiver which is co-located with the transmitter) for the T-N and T-W configurations, corroborates the conclusion drawn from Figure 1; namely, that the induced signal along the longitudinal axis is much larger than that along the transverse axis. To see this, recall that for the T-N configuration, the primary field directly below the sensor is along the longitudinal axis, while for both the T-B and T-W configurations, the primary field is along the transverse axes. Since the distance from the center of the transmitter coil to the center of the target is comparable for the T-N and T-W cases, we can directly compare these two signal strengths and arrive at the above-stated conclusion.

Our model assumes that a uniform field excites the target, with a magnitude given by the value of the primary field at the center of the target. In reality, however, a variation exists for the primary field over the extent of the target. This variation is found to be small (~1.5%) for the T-B configuration over the extent of the 2.75" rocket, but 3 and 4 times larger for the T-N and T-W configurations, respectively. This, along with contributions from higher-order moments, most likely explains the discrepancies observed in Figure 4(e)-(f). The important point here is that, regardless of the primary field variations and near field effects, the model still does remarkably well.

Spatial data collected for the shovel blade (lying flat, with pointed end facing east) is shown in Figure 5. The solid lines again represent the best model fit to the data. In this case, the parameters correspond to a slightly prolate target with an induced field ratio of 1.85 . The dashed lines represent the best model fit to the data if one confines the target to have an induced field ratio less than 1. It is interesting to note the similarities between the two sets of curves.

The fact that these two sets of curves are so similar suggests that shape classification based solely on field ratios is too simplistic. However, since the shovel blade (which includes a cylindrical projection by which it can be attached to a handle) is irregularly shaped, the tensor in (2) is no longer an appropriate representation for the induced fields, and so the mismatch between model and data now becomes important in discriminating between regular (i.e. UXO) and irregular (i.e. clutter) shapes. This mismatch is embodied in the minimum χ^2 surface.

Recall that we fit our model to the data via a χ^2 minimization procedure. The topology of the minimum χ^2 surface determines how well the model parameters can be estimated. This surface, as a function of target orientation angles, θ and φ (defined here as the standard inclination and azimuth angles of the spherical coordinate system), describes how the minimum χ^2 varies. The minimum χ^2 value is obtained for each θ and φ by determining the β_l and β_t coefficients for which χ^2 is a minimum. Figure 6 shows four such normalized surfaces.

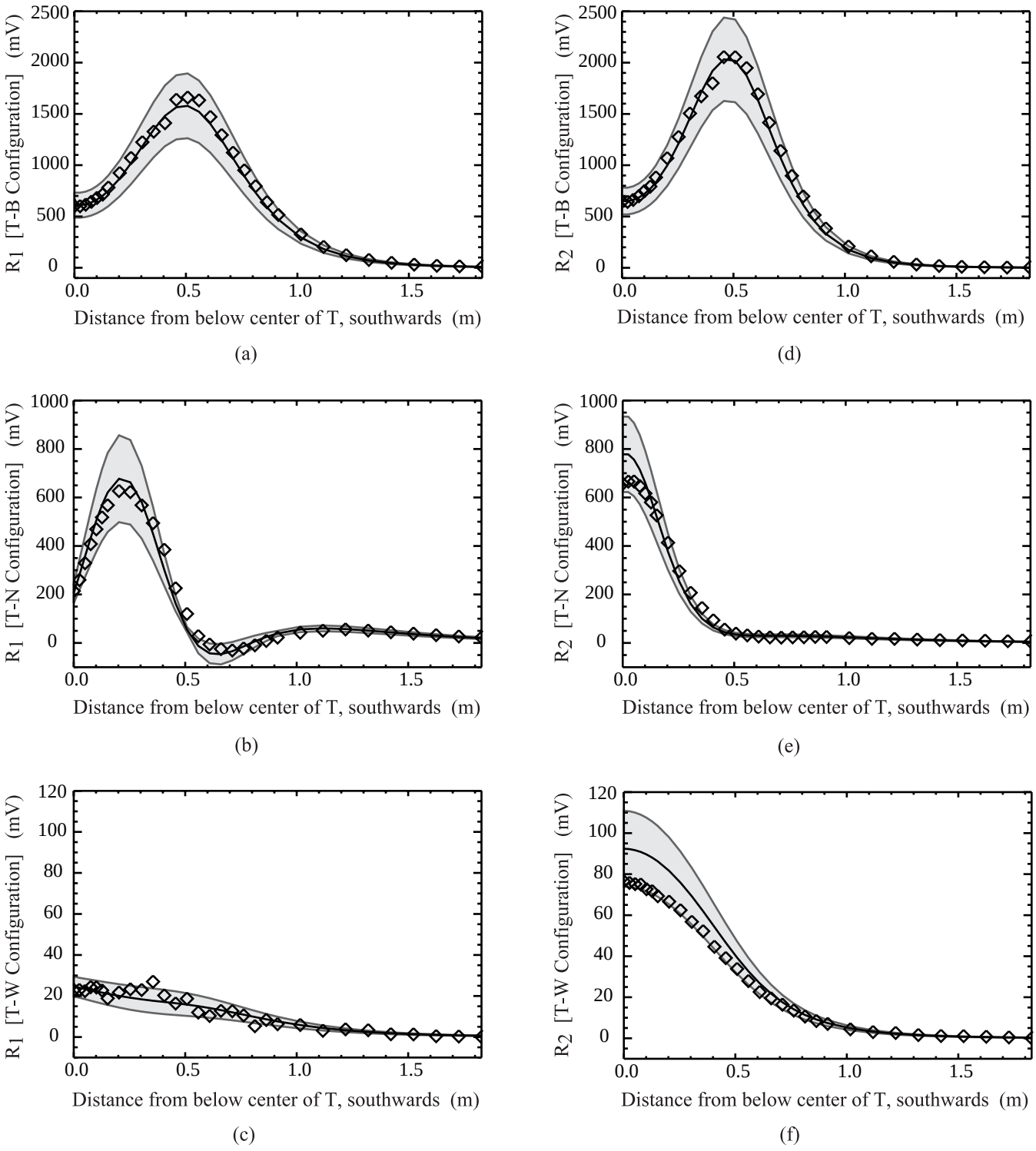

Figure 4. EM61 spatial data collected for the 2.75" rocket (long axis facing northwards) with the three sensor configurations (T-B, T-N and T-W). The diamond symbols represent the measured averaged values; the solid line represents the best model fit. The shaded region shows the consequence of varying the β_l and β_t parameters by as much as ±20%.

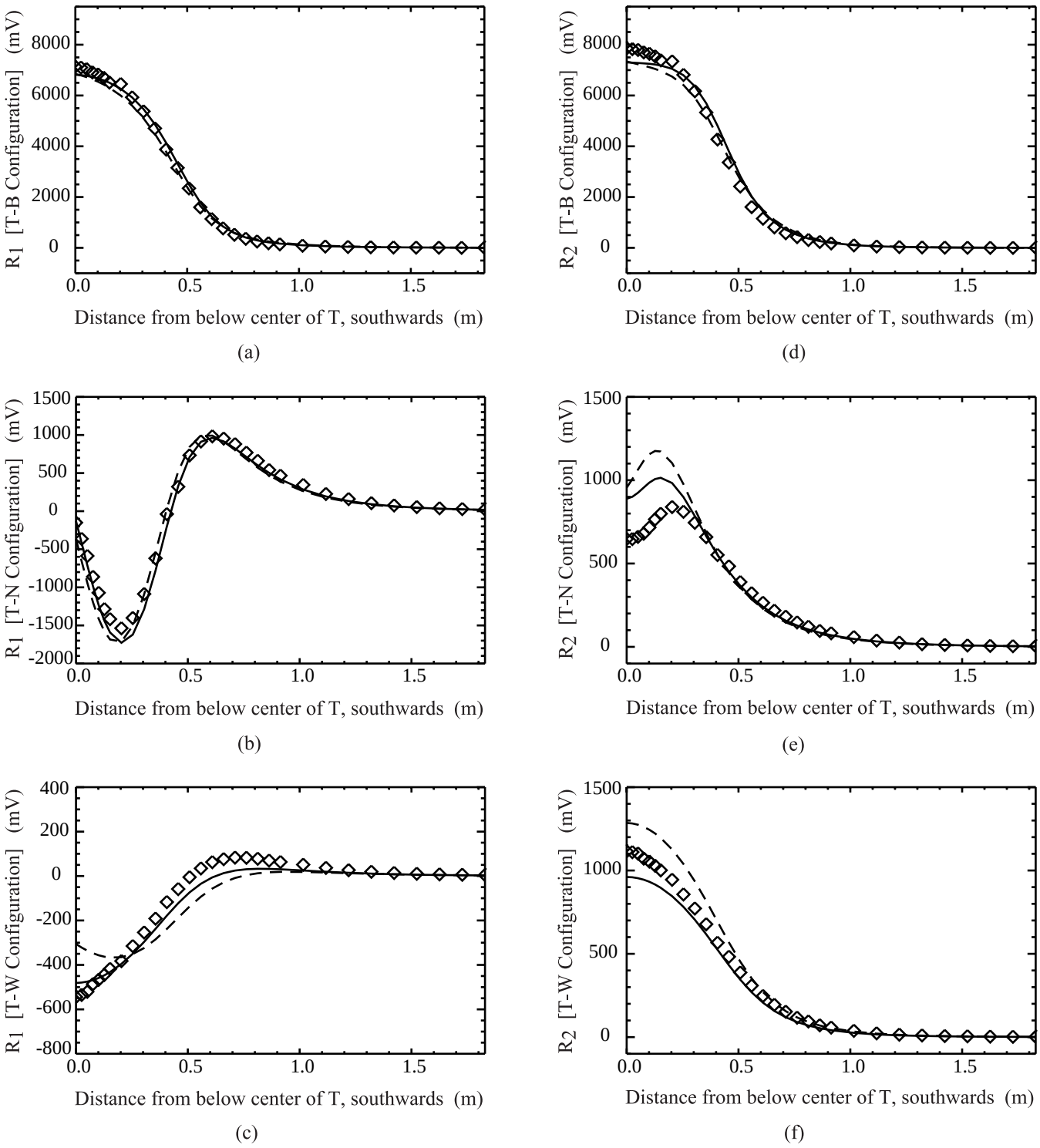

Figure 5. EM61 spatial data collected for the shovel blade (lying flat, pointed end facing east) with the three sensor configurations (T-B, T-N and T-W). The diamond symbols represent the measured averaged values; the solid line represents the best model fit (prolate solution); and the dashed line represents the best oblate solution.

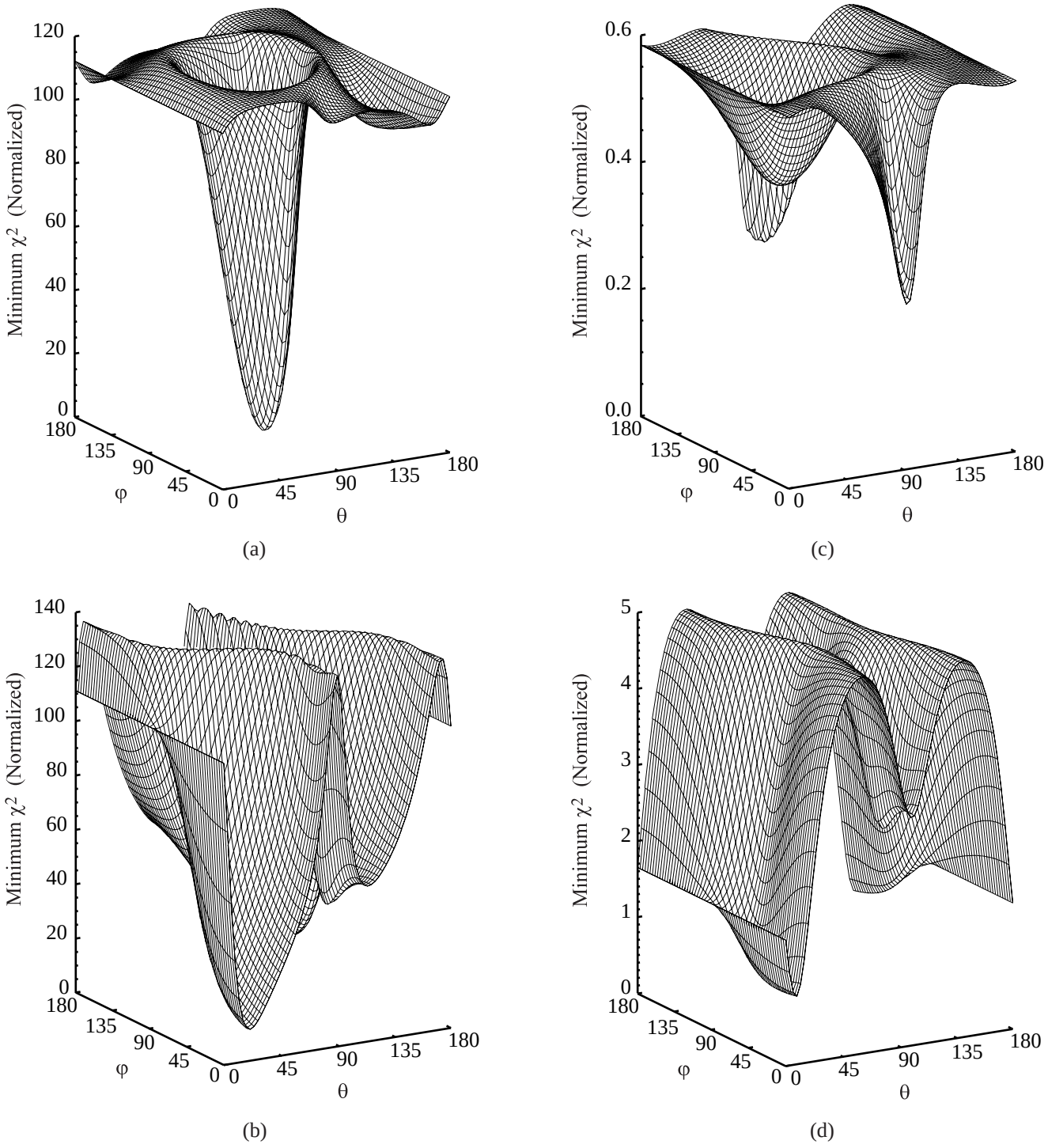

Figure 6. Minimum χ^2 surfaces for the (a) 2.75" rocket; (b) Shovel blade; (c) Clump of banding material; and (d) Flattened soda can.

It is clear that the surface for the 2.75" rocket (Figure 6(a)) is well behaved compared to the three other surfaces representing various clutter items (Figure 6(b)-(d)). As is the case for our standard test objects (i.e. disks and cylinders), the χ^2 minimum for the 2.75" rocket is very well defined and occurs to within a degree or two of the actual target orientation. The same, however, cannot be said for the clutter items. Here, several minima exist creating a certain ambiguity in the parameter estimation procedure. This was observed for the shovel blade, where the data in Figure 5 was feasibly represented by both the prolate and oblate solutions.

CONCLUSION

Most UXO items are long and slender, with typical length-to-diameter aspect ratios of four or five. When probed by an EMI sensor, the ratios of the axially induced fields to the transversely induced fields, in this case, are determined to be larger than 1. More importantly, our simple model embodied in (1) and (2) represents the fields very well.

Most clutter items are *not* long and slender. They are either flat and regularly shaped, or irregularly shaped. When flat and regular, our simple model still represents the fields very well, but now the resulting induced field ratios are less than 1. When irregular, however, information based on the ambiguity of our simple model with respect to the data is essential for proper classification. This information is manifested in the topology of the minimum χ^2 surface.

ACKNOWLEDGEMENTS

The authors would like to thank Larry Koppe for his invaluable efforts in the data collection process.

REFERENCES

[1] Office of the Undersecretary of Defense (Acquisition and Technology), "Report to Congress: Unexploded Ordnance Clearance," pp. 25-26, March 1977.

[2] Barrow, B., R. DiMarco, N. Khadr and H. H. Nelson, "Processing and analysis of UXO signatures measured with MTADS," Proc. UXO Forum 1997, pp. 8-18, May 1997.

[3] Das, Y., J. E. McFee, J. Toews and G. C. Stuart, "Analysis of an Electromagnetic Induction Detector for Real-Time Location of Buried Objects," IEEE Transactions on Geoscience and Remote Sensing, **28**, pp. 278-287, 1990.